Journal of Alloys and Compounds 513 (2012) 324–327

Contents lists available at SciVerse ScienceDirect

Journal of Alloys and Compounds

journal homepage: www.elsevier.com/locate/jallcom

Mechanochemical transformations in $NaNH_2$-MgH_2 mixtures

Niraj K. Singh[a], Takeshi Kobayashi[a], Oleksandr Dolotko[a], Jerzy W. Wiench[a], Marek Pruski[a,b,*], Vitalij K. Pecharsky[a,c]

[a] *Ames Laboratory, Iowa State University, Ames, IA 500011-3020, USA*
[b] *Department of Chemistry, Iowa State University, Ames, IA 500011-3111, USA*
[c] *Department of Materials Science and Engineering, Iowa State University, Ames, IA 50011-2300, USA*

ARTICLE INFO

Article history:
Received 12 July 2011
Received in revised form 8 October 2011
Accepted 10 October 2011
Available online 24 October 2011

Keywords:
Hydrogen storage
Mechanochemical transformation
Solid-state NMR
X-ray diffraction

ABSTRACT

Mechanochemical transformations occurring during ball milling of sodium amide ($NaNH_2$) with magnesium hydride (MgH_2) taken in 2:3 and 2:1 molar ratios have been investigated using X-ray powder diffraction (XRD) and solid-state nuclear magnetic resonance (SSNMR) techniques. For the $2NaNH_2$–$3MgH_2$ system the mechanochemical reaction proceeds via the formation of MgNH as an intermediate, whereas magnesium nitride (Mg_3N_2), sodium hydride (NaH) and hydrogen (~5 wt%) form as the final products. The overall solid state reaction for this system is $2NaNH_2 + 3MgH_2 \rightarrow Mg_3N_2 + 2NaH + 4H_2$. However, the mechanochemical transformation of the $2NaNH_2$–MgH_2 system proceeds through the reaction: $2NaNH_2 + MgH_2 \rightarrow Mg(NH_2)_2 + 2NaH$, without any hydrogen release. Comparison of the mechanochemical transformations with the previously studied thermochemical transformations reveals that the two approaches lead to the same final products via different reaction pathways.

1. Introduction

Continuously increasing demand for energy stimulates the exploration of alternative energy sources, and in this context various solid-state hydrogen storage materials have been examined [1,2]. Among these, complex hydrides formed with lightweight alkali metals, such as lithium and sodium, have attracted considerable attention mainly due to their high gravimetric hydrogen content [1,3,4]. Recently, Chen et al. [5] reported that hydrogenation of lithium nitride (Li_3N) and subsequent dehydrogenation can be performed via the following reversible two-step reaction:

$$Li_3N + 2H_2 \leftrightarrow Li_2NH + LiH + H_2 \leftrightarrow LiNH_2 + 2LiH \quad \text{(R1)}$$

Theoretically, as much as 10.4 wt% of hydrogen can be stored using this system. However, the strongly endothermic nature of the above reaction requires high operation temperature, which hinders practical application of this $LiNH_2$–LiH system.

Subsequently, Nakamori and Orimo [6] reported that replacement of Li by an element with higher electronegativity, such as Mg, improves the dehydrogenation properties of $LiNH_2$. Later studies involved mechanochemistry and thermochemistry of various mixtures of $LiNH_2$ and MgH_2 [7–17]. Luo [7] and Xiong et al. [8] independently demonstrated that the replacement of LiH by MgH_2 affects the dehydrogenation properties, and 4.5 wt% of hydrogen can be reversibly stored in the $2LiNH_2$–MgH_2 mixture. The thermal dehydrogenation of this system leads to the formation of $Li_2Mg(NH)_2$ through the first step of reaction (R2) [7,8]. However, the hydrogenation of $Li_2Mg(NH)_2$ leads to the formation of $Mg(NH_2)_2$ and LiH through the second step of (R2), and it is this step of the reaction which is responsible for the reversibility of hydrogen in the $2LiNH_2$–MgH_2 system [8–11]

$$2LiNH_2 + MgH_2 \rightarrow Li_2Mg(NH)_2 + 2H_2\uparrow \leftrightarrow Mg(NH_2)_2 + 2LiH \quad \text{(R2)}$$

The ball milling of the same system yields directly $Mg(NH_2)_2$ and 2LiH [11–13], which demonstrates that reactions induced by mechanical energy may proceed through nonequilibrium configurations with different final products. A similar discrepancy was recently reported in $2LiNH_2$–CaH_2 system, which under thermochemical conditions decomposes to $Li_2Ca(NH)_2$ and can be hydrogenated to $Ca(NH_2)_2$ and LiH, in analogy to (R2) [18]. However, neither $Li_2Ca(NH)_2$ nor $Ca(NH_2)_2$ is formed during mechanical milling of $2LiNH_2$–CaH_2 mixture [19].

Two recent reports focused on thermal decomposition of the mixture of MgH_2 and sodium amide, $NaNH_2$ [20,21]. In the $2MNH_2$–$3MgH_2$ system (M = Li or Na) studied by Dolotko et al. [20], the dehydrogenation proceeds according to

$$2MNH_2 + 3MgH_2 \rightarrow Mg_3N_2 + 2MH + 4H_2\uparrow \quad \text{(R3)}$$

Although the final products are the same, different intermediates arise for M = Li ($Li_2Mg(NH)_2$) and M = Na ($Mg(NH_2)_2$ and $NaMgH_3$). The attempt of hydrogenation of the decomposed

---

* Corresponding author at: Ames Laboratory, Iowa State University, Ames, IA 500011-3020, USA. Tel.: +1 515 294 2017.
E-mail address: mpruski@iastate.edu (M. Pruski).

0925-8388/$ – see front matter © 2011 Elsevier B.V. All rights reserved.
doi:10.1016/j.jallcom.2011.10.041

products for M = Li was unsuccessful [20]. However, in the case of M = Na, partial rehydrogenation has been observed:

$$Mg_3N_2 + 2NaH + 2H_2 \rightarrow 2MgNH + 2NaH + MgH_2 \qquad (R4)$$

Most recently, hydrogen desorption from $LiNH_2$–MgH_2 mixture (1:1) has been reported [21], which yields 3.3 wt% between 70 and 335 °C. The temperature programmed dehydrogenation curve was different than that reported by Dolotko et al. [20], and two new, unidentified magnesium-containing phases corresponding to an imide and nitride were involved in the decomposition pathway.

Herein, we describe the solid-state transformations occurring during mechanical milling of two mixtures of $NaNH_2$ and MgH_2. In view of the aforementioned differences between thermochemical and mechanochemical transformations in other hydride systems, we re-examined the $2NaNH_2$–$3MgH_2$ mixture, which indeed produces a new intermediate (MgNH). We have also investigated the previously unexplored $2NaNH_2$–MgH_2 system. Our earlier studies have demonstrated that in order to properly characterize the crystalline and amorphous phases of reacting hydrides, such studies can be best performed by combining the X-ray powder diffraction (XRD) and solid-state nuclear magnetic resonance (SSNMR) spectroscopy [22,23].

2. Experimental details

2.1. Materials and mechanochemical processing

The starting materials $NaNH_2$ (>90 wt% purity) and NaH (>95 wt% purity) used in this study were purchased from Sigma–Aldrich, whereas MgH_2 (>98 wt% purity) was purchased from Alfa-Aesar. Due to the air sensitivity of the starting materials and the products, all manipulations have been carried out under a continuously purified and monitored argon atmosphere in a glove box.

About 1 g of the intended mixture was loaded in a 50 ml hardened-steel vial and ball milled using 20 g of steel balls (2 large balls weighing 8 g each and 4 small balls weighing 1 g each) in an 8000 M SPEX mill. The samples, henceforth referred to as $NaNH_2$–MgH_2(sm), where ‘sm’ denotes the ‘starting mixture’, and $NaNH_2$–MgH_2(time), were analyzed as a function of ball milling time. The reference compound $NaMgH_3$ was synthesized by ball milling of 1 g of 1:1 mixture of NaH and MgH_2 in a SPEX mill for 3 h.

2.2. X-ray powder diffraction analysis

Reaction products were characterized by X-ray powder diffraction analysis at room temperature on a PANalytical powder diffractometer using Cu Kα radiation with a 0.02° 2θ step, in the range of Bragg angles 2θ from 10° to 80°. During the measurements a polyimide (Kapton) film was used to protect the samples from air. The use of film resulted in an amorphous like background in the XRD patterns in the 2θ range of 13–20°.

2.3. Solid-state NMR analysis

The ^{1}H and ^{23}Na solid-state NMR experiments were performed at 14.1 T on a Varian NMR System spectrometer, equipped with a triple tuned 1.6 mm T3 magic angle spinning (MAS) probe operating at a rate of 25 kHz. The ball milled samples and reference compounds were packed in MAS zirconia rotors in a glove box under argon atmosphere and tightly capped to avoid oxygen and moisture contamination. The one-dimensional spectra were acquired using a single pulse excitation, a radio frequency (RF) magnetic field of approximately 80 kHz, a small flip angle of 15° for quantitative accuracy (in the case of ^{23}Na) and ^{1}H TPPM (Two-Pulse Phase-Modulated) decoupling [24] at 104 kHz during acquisition. The recycle delays were 60 s for ^{1}H and 1 s for ^{23}Na. The ^{1}H and ^{23}Na shifts were referenced to tetramethylsilane (TMS) and 1.0 M aqueous solutions of NaCl, respectively, at 0 ppm.

3. Results and discussion

The transformations of $2NaNH_2$–$3MgH_2$ and $2NaNH_2$–MgH_2 mixtures were monitored by analyzing the XRD patterns and solid-state NMR spectra of samples ball milled for up to 18 h and 15 h, respectively, which sufficed to complete the reactions. The milling of 2:3 molar mixtures leads to the development of pressure in the vial and, as confirmed by residual gas analysis, pure hydrogen was observed as the gaseous product resultingfrom the mechanochemical transformations. During the milling of 2:1 mixture no pressure was developed in the vial, which indicates that the mechanochemical changes do not involve formation of any gaseous products.

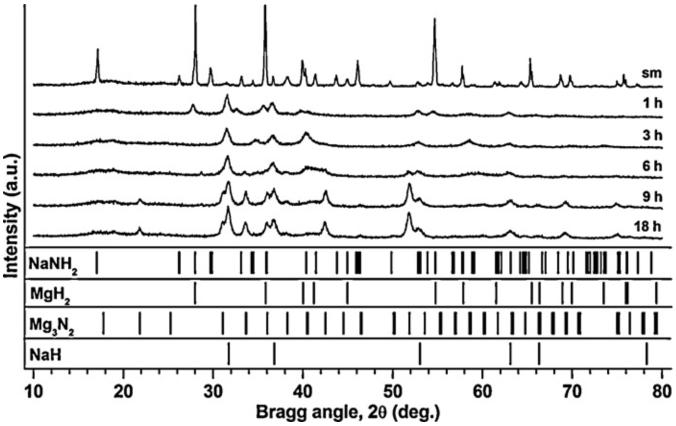

Fig. 1. The XRD patterns of the $2NaNH_2$–$3MgH_2$ mixture, reaction products after ball milling and reference compounds. Only the locations (but not intensities) of the Braggs peaks of the starting compounds and two reaction products are shown as the vertical markers at the bottom of the plot. Braggs peaks of the intermediate (MgNH) are observed at 2θ = 34.7°, 40.8°, and 59.3° in samples after 1, 3, and 6 h of processing.

3.1. XRD studies

Fig. 1 shows the XRD patterns collected on $2NaNH_2$–$3MgH_2$(sm) and samples milled for 1, 3, 6, 9 and 18 h. Besides the Bragg reflections corresponding to the starting materials, the pattern of $2NaNH_2$–$3MgH_2$(1 h) sample shows the presence of NaH and a new set of reflections at 2θ = 34.7°, 40.8° and 59.3°, which are consistent with those assigned to MgNH [25,26]. With increase in the milling time to 3 h the contribution from the starting materials diminishes whereas the Bragg reflections corresponding to NaH and MgNH become more pronounced. In the $2NaNH_2$–$3MgH_2$(6 h) sample the reflections due to NaH and MgNH are still present; however, the intensities corresponding to MgNH decrease and a new set of Bragg reflections corresponding to Mg_3N_2 becomes visible. At 9 h this set becomes prominent, whereas the reflections corresponding to NaH remain and the peaks from MgNH vanish. The milling of the mixture for 18 h does not yield any additional reflections, which indicates that the mechanochemical transformation for the $2NaNH_2$–$3MgH_2$ system is completed in less than 9 h.

Fig. 2 shows a similar series of XRD patterns for the $2NaNH_2$–MgH_2 system. While the sample milled for 1 h ($2NaNH_2$–MgH_2(1 h)) shows Bragg reflections representing only the starting materials, the characteristic peaks corresponding to $Mg(NH_2)_2$ and NaH appear in the $2NaNH_2$–MgH_2(3 h) sample. Further increase in the milling time to 6 h results in lowering of the intensity of the Bragg peaks corresponding to the starting materials whereas the intensities due to $Mg(NH_2)_2$ and NaH increase. After 9, 12 and 15 h of ball milling, only the peaks representing $Mg(NH_2)_2$ and NaH are observed. Thus, the XRD data suggest that the mechanochemical transformation of the $2NaNH_2$–MgH_2 system is also completed in 9 h or less, leading to the final products $Mg(NH_2)_2$ and NaH in a single step with no detectable intermediates.

3.2. Solid-state NMR studies

In addition to the XRD analysis, the ^{23}Na and ^{1}H solid-state NMR measurements were performedon the similar sets

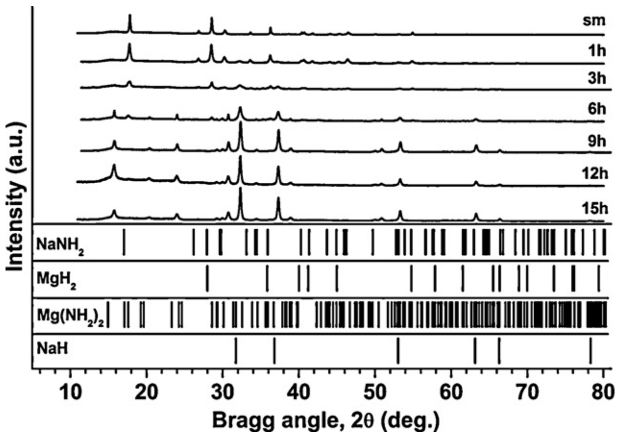

Fig. 2. The XRD patterns of the $2NaNH_2$–MgH_2 mixture, reaction products after ball milling and reference compounds. Only the locations (but not intensities) of the Braggs peaks of the starting compounds and two reaction products are shown as the vertical markers at the bottom of the plot.

of samples. For the $2NaNH_2$–$3MgH_2$ system, we measured the spectra of $2NaNH_2$–$3MgH_2$(3 h), $2NaNH_2$–$3MgH_2$(10 h) and $2NaNH_2$–$3MgH_2$(18 h), as well as several reference compounds. The spectra of the starting materials, MgH_2 and $NaNH_2$, are shown in Fig. 3a and b, respectively. Also shown are the results obtained for NaH (Fig. 3c), $NaMgH_3$ (Fig. 3d), the starting (physical) mixture of $NaNH_2$ and MgH_2 (Fig. 3e), and sample $2NaNH_2$–$3MgH_2$(3 h). The spectra of samples $2NaNH_2$–$3MgH_2$(10 h) and $2NaNH_2$–$3MgH_2$(18 h) were identical with those of $2NaNH_2$–$3MgH_2$(3 h), and thus are not reported.

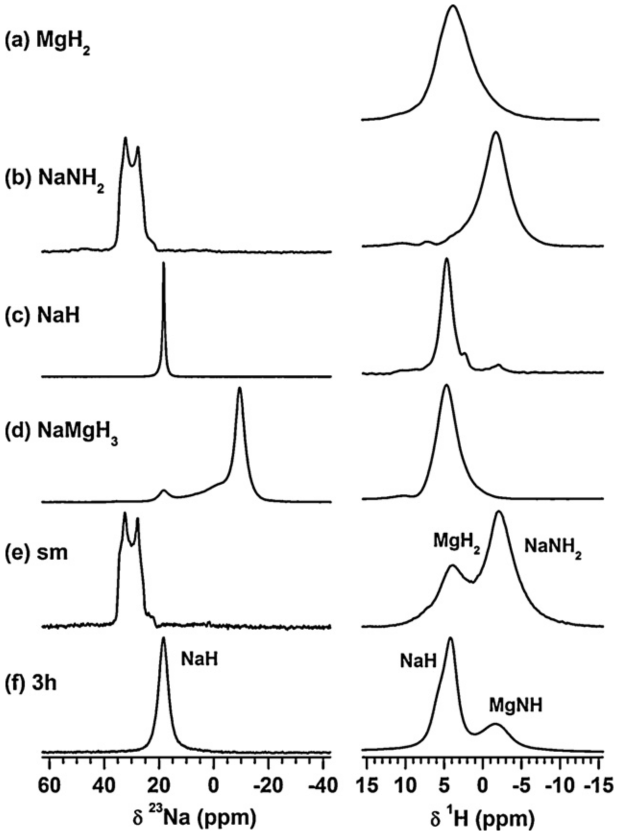

Fig. 3. ^{23}Na and ^{1}H MAS NMR spectra of the reference compounds, the physical mixture $NaNH_2$-MgH_2(sm), and sample $2NaNH_2$-$3MgH_2$(3h).

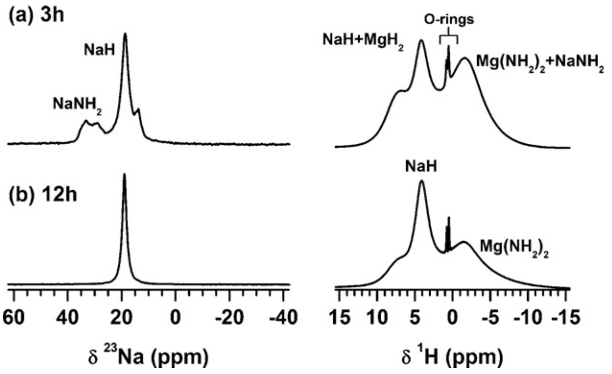

Fig. 4. ^{23}Na and ^{1}H MAS NMR spectra of samples $2NaNH_2$-MgH_2(3h) and $2NaNH_2$-MgH_2(12 h).

The results of NMR measurements agree well with the XRD analysis. After 3 h of ball milling, sodium amide, whose ^{23}Na spectrum exhibits a characteristic second order powder pattern in Fig. 3e [27,28], is completely transformed into NaH (compare the ^{23}Na spectra in Fig. 3f and c). Clearly, NaH represents the only final product of the reaction that contains sodium. The analysis of ^{1}H spectra is more difficult due to small chemical shift range and considerable line broadening caused by strong ^{1}H–^{1}H dipolar interactions. As expected, the ^{1}H spectrum of the starting mixture (Fig. 3e) is a superposition of the spectra of individual reactants (Fig. 3a and b). However, while both ^{1}H resonances observed in sample $2NaNH_2$–$3MgH_2$(3 h) appear at similar frequencies to the starting mixture, they represent different species. Indeed, the peak at ∼−2 ppm cannot result from sodium amide and thus is assigned to MgNH, which should resonate in the same frequency range. The newly formed NaH should yield a ^{1}H resonance at ∼4 ppm, as is indeed observed in Fig. 3f. A small shoulder observed on the high-frequency side of this peak is due to background from the spacers located inside the MAS rotor.

Fig. 4a and b shows the ^{23}Na and ^{1}H solid-state NMR spectra of samples $2NaNH_2$–MgH_2(3 h) and $2NaNH_2$–MgH_2(12 h). The dominant ^{23}Na resonances in Fig. 4a represent unreacted $NaNH_2$ and NaH product, as indicated in the spectrum. In addition, a small amount of unidentified, sodium-containing intermediate is found in this sample, represented by the ^{23}Na peak at ∼13 ppm. Similarly to the $2NaNH_2$–$3MgH_2$ system, the ^{1}H spectrum of sample $2NaNH_2$–MgH_2(3 h) is dominated by two peaks at ∼4 ppm and ∼−1.5 ppm. The first peak can be easily assigned to NaH, whereas the one at ∼−1.5 ppm is most likely a superposition of resonances representing $Mg(NH_2)_2$ and unreacted $NaNH_2$. (Although we were not able to obtain a suitable $Mg(NH_2)_2$ reference, the ^{1}H shift in this compound should be similar to one observed for $NaNH_2$ in Fig. 3b.) The dominant ^{1}H resonances in Fig. 4b are consistent with NaH and $Mg(NH_2)_2$ being the final products of decomposition. The sharp ^{1}H peaks around 0.5 ppm originate from the silicon rubber in the O-rings used to seal the MAS rotor, which were not used while collecting the spectra of Fig. 3. Again, the broad shoulder on the high-frequency side of the spectrum is due to the MAS rotor background. The contribution to this peak from intermediate species cannot be ruled out, at least in sample $2NaNH_2$–MgH_2(3 h).

3.3. Transformation mechanism

The mechanochemical transformation of $NaNH_2$ and MgH_2 taken in a 2:3 molar ratio appears to proceed in two steps. In the first step, which is similar to the $LiNH_2 + MgH_2$ system [17], $NaNH_2$ and MgH_2 react to form MgNH and release hydrogen through (R5).

In the second step MgNH reacts with the remaining MgH_2, and Mg_3N_2 is formed through (R6):

$$NaNH_2 + MgH_2 \rightarrow NaH + MgNH + H_2 \tag{R5}$$

$$2MgNH + MgH_2 \rightarrow Mg_3N_2 + 2H_2 \tag{R6}$$

In the abovementioned reaction path, only MgNH was observed as an intermediate species. Since the system contains NaH and MgH_2 after the first step, the formation of $NaMgH_3$ could be expected during ball milling [29]. However, this possibility was ruled out by comparing the ^{23}Na NMR spectra of the final products with the specially prepared $NaMgH_3$ reference (Fig. 3d and f). Thus, the overall mechanochemical transformation reaction for the $2NaNH_2$–$3MgH_2$ system can be written as:

$$2NaNH_2 + 3MgH_2 \rightarrow 2NaH + Mg_3N_2 + 4H_2 \tag{R7}$$

We note that the mechanochemical transformation of $2NaNH_2 + 3MgH_2$ system proceeds differently than the thermochemical process [20], despite the final products being the same. During the thermal decomposition of $2NaNH_2 + 3MgH_2$ mixture, $Mg(NH_2)_2$ and $NaMgH_3$ are observed as intermediates, whereas only MgNH is detected as the intermediate product during mechanochemical reaction. These observations indicate that, in contrast to thermochemical transformations, which proceed in accordance with thermodynamic equilibrium, the reactions induced by mechanical energy may drive the reaction through nonequilibrium configurations leading to formation of different intermediate species [19].

Based on the XRD and NMR data and the fact that no hydrogen is released during the ball milling, the mechanochemical transformation for the $2NaNH_2$–MgH_2 mixture can be written as

$$2NaNH_2 + MgH_2 \rightarrow Mg(NH_2)_2 + 2NaH \tag{R8}$$

A similar metathesis reaction has been also reported for the mechanochemical decomposition of the $2LiNH_2$–MgH_2 system [11,12]. However, the NMR spectra of sample $2NaNH_2$–MgH_2(3 h) suggest that this reaction may involve an intermediate, yet to be identified step.

4. Conclusions

The effect of ball milling on 2:3 and 2:1 mixtures of $NaNH_2$ and MgH_2 has been investigated by the combined use of XRD and SSNMR spectroscopy. For the 2:3 system, pure hydrogen is released and the reaction proceeds in two steps. In the first step, $NaNH_2$ and MgH_2 react to yield MgNH and NaH through the reaction $NaNH_2 + MgH_2 \rightarrow NaH + MgNH + H_2$, whereas in the second step MgNH reacts with the remaining MgH_2 and transforms to Mg_3N_2 via the reaction $2MgNH + MgH_2 \rightarrow Mg_3N_2 + 2H_2$. The overall mechanochemical reaction for 2:3 mixture is $2NaNH_2 + 3MgH_2 \rightarrow 2NaH + Mg_3N_2 + 4H_2$. In case of the 2:1 mixture, no gaseous hydrogen is released during the milling, and the mechanochemical transformation involves a metathesis reaction $2NaNH_2 + MgH_2 \rightarrow Mg(NH_2)_2 + 2NaH$.

Acknowledgements

This work was supported by the Office of Basic Energy Sciences of the Office of Science of the U.S. Department of Energy under contract No. DE-AC02-07CH11358 with Iowa State University of Science and Technology.

References

[1] S.I. Orimo, Y. Nakamori, J.R. Eliseo, A. Zuttel, C.M. Jensen, Chem. Rev. 107 (2007) 4111–4132.
[2] B. Sakintuna, F. Lamari-Darkrim, M. Hirscher, Int. J. Hydrogen Energy 32 (2007) 1121–1140.
[3] J.J. Vajo, G.L. Olson, Scripta Mater. 56 (2007) 829–834.
[4] F. Schuth, B. Bogdanovic, M. Felderhoff, Chem. Commun. 224 (2004) 9–2258.
[5] P. Chen, Z.T. Xiong, J.Z. Luo, J.Y. Lin, K.L. Tan, Nature 420 (2002) 302–304.
[6] Y. Nakamori, S. Orimo, Mater. Sci. Eng. B 108 (2004) 48–50.
[7] W.F. Luo, J. Alloys Compd. 381 (2004) 284–287.
[8] Z.T. Xiong, G.T. Wu, H.J. Hu, P. Chen, Adv. Mater. 16 (2004) 1522–1525.
[9] W.F. Luo, S. Sickafoose, J. Alloys Compd. 407 (2006) 274–281.
[10] Y. Chen, C.Z. Wu, P. Wang, H.M. Cheng, Int. J. Hydrogen Energy 31 (2006) 1236–1240.
[11] S. Barison, F. Agresti, S. Lo Russo, A. Maddalena, P. Palade, G. Principi, G. Torzo, J. Alloys Compd. 459 (2008) 343–347.
[12] R.R. Shahi, T.P. Yadav, M.A. Shaz, O.N. Srivastava, Int. J. Hydrogen Energy 33 (2008) 6188–6194.
[13] K. Tokoyoda, S. Hino, T. Ichikawa, K. Okamoto, H. Fujii, J. Alloys Compd. 439 (2007) 337–341.
[14] H.Y. Leng, T. Ichikawa, S. Hino, T. Nakagawa, H. Fujii, J. Phys. Chem. B 109 (2005) 10744–10748.
[15] W. Osborn, T. Markmaitree, L.L. Shaw, J. Power Sources 172 (2007) 376–378.
[16] Y.F. Liu, K. Zhong, M.X. Gao, H.H. Wang, H.G. Pan, Q.D. Wang, Chem. Mater. 20 (2008) 3521–3527.
[17] C. Liang, Y.F. Liu, K. Luo, B. Li, M.X. Gao, H.G. Pan, Q.D. Wang, Chem. Eur. J. 16 (2010) 693–702.
[18] G.T. Wu, Z.T. Xiong, T. Liu, Y.F. Liu, J.J. Hu, P. Chen, Y.P. Feng, A.T.S. Wee, Inorg. Chem. 46 (2007) 517–521.
[19] O. Dolotko, H.Q. Zhang, S. Li, P. Jena, V. Pecharsky, J. Alloys Compd. 506 (2010) 224–230.
[20] O. Dolotko, N. Paulson, V.K. Pecharsky, Int. J. Hydrogen Energy 35 (2010) 4562–4568.
[21] D.A. Sheppard, M. Paskevicius, C.E. Buckley, J. Phys. Chem. C 115 (2011) 8407–8413.
[22] V.P. Balema, J.W. Wiench, K.W. Dennis, M. Pruski, V.K. Pecharsky, J. Alloys Compd. 329 (2001) 108–114.
[23] O. Dolotko, H.Q. Zhang, O. Ugurlu, J.W. Wiench, M. Pruski, L.S. Chumbley, V. Pecharsky, Acta Mater. 55 (2007) 3121–3130.
[24] A.E. Bennett, C.M. Rienstra, M. Auger, K.V. Lakshmi, R.G. Griffin, J. Chem. Phys. 103 (1995) 6951–6958.
[25] S. Hino, T. Ichikawa, Y. Kojima, J. Chem. Thermodyn. 42 (2010) 140–143.
[26] J.J. Hu, G.T. Wu, Y.F. Liu, Z.T. Xiong, P. Chen, K. Murata, K. Sakata, G. Wolf, J. Phys. Chem. B 110 (2006) 14688–14692.
[27] A. Abragam, Principles of Nuclear Magnetism, Oxford University Press, New York, 1986.
[28] K. Narita, J.I. Umeda, H. Kusumoto, J. Chem. Phys. 44 (1966) 2719–2723.
[29] K. Ikeda, Y. Nakamori, S. Orimo, Acta Mater. 53 (2005) 3453–3457.